

X-ray Spectral Survey of WGACAT Quasars, I: Spectral Evolution & Low Energy Cut-offs

Fabrizio Fiore^{1,2,3}, Martin Elvis¹, Paolo Giommi³,
Paolo Padovani⁴

¹ Harvard-Smithsonian Center for Astrophysics
60 Garden St, Cambridge MA 02138

²Osservatorio Astronomico di Roma, Monteporzio (Rm), Italy

³BeppoSAX Science Data Center, Roma, Italy

⁴Dipartimento di Fisica, II Università di Roma

version: 1pm June 24 1997

ABSTRACT

We have used the WGA catalog of ROSAT PSPC X-ray sources to study the X-ray spectrum of about 500 quasars in the redshift interval 0.1–4.1, detected with a signal to noise better than 7. We have parameterized the PSPC spectrum in terms of two ‘effective energy spectral indices’, α_S (0.1–0.8 keV), and α_H (0.4–2.4 keV), which allows for the different Galactic N_H along the quasars line of sight. We have used these data to explore the questions raised by the initial PSPC high redshift quasar studies, and in particular the occurrence of low X-ray energy cut-offs in high redshift radio-loud quasars. We have also studied the emission spectra of a large sample of radio-loud and radio-quiet quasars and studied their differences.

We find that low energy X-ray cut-offs are more commonly (and perhaps exclusively) found in radio-loud quasars. Therefore the low energy X-ray cut-offs are physically associated with the quasars, and not with intervening systems, since those would affect radio-quiet and radio-loud equally. We suggest that photoelectric absorption is a likely origin of the these cut-offs.

The number of ‘cut-offs’ in radio-loud quasars significantly increases with redshift, rather than with luminosity. A partial correlation analysis confirms that α_S is truly anti-correlated with redshift at the 99.9% confidence level, indicating evolution with cosmic epoch, and not a luminosity effect. Conversely, for α_H the observed anti-correlation with redshift is mostly due to a strong dependence on luminosity.

We find marginal evidence for a flattening of α_H (P=4.5 %) going from $z < 1$ to $z = 2$, in radio-quiet quasars, in agreement with previous studies. On the other

hand, radio-loud quasars at $z < 2.2$ show a ‘concave’ spectrum ($\alpha_H < \alpha_S$ by ~ 0.2). This new result is consistent with the widespread suggestion that the X-ray spectrum of radio-loud quasars may be due to an additional component above that seen in radio-quiet quasars. However, it might also imply different processes at work in radio-loud and radio-quiet sources. At $z \gtrsim 2$ the average soft and hard indices are similar and both significantly smaller than at lower redshifts. This can be due to the soft component of radio-loud quasars being completely shifted out of the PSPC band at $z > 2$.

Subject headings: quasars — absorption, quasar — evolution, X-rays

1. Introduction

The ability of ROSAT to study fainter X-ray sources than ever before opened up the range of quasars that could be reached to span virtually the whole of their properties. High redshift objects (up to $z \approx 4$) became accessible in X-rays, and their spectrum was measured for the first time between 0.4 and 10 keV (in the quasar frame, Elvis et al 1994a). Unexpected low energy cut-offs, far larger than those expected due to absorption by our galaxy, were detected in several high- z radio-loud quasars (Wilkes et al. 1993, Elvis et al. 1994a). The obvious possibility was that these were caused by photoelectric absorption, either along the line of sight, or at the quasar. If the absorber were at the quasar, then the material could be nuclear, as in low redshift low luminosity objects (e.g. Elvis & Lawrence, 1985, and Elvis, Mathur & Wilkes 1995) or could be on the larger scale of the host galaxy or proto-galaxy. A tentative link with the highly compact ‘GigaHertz Peaked’ (GPS) radio sources suggested the latter and hence that X-ray astronomy offered a new probe of early galaxy conditions.

Targeted ROSAT studies of high redshift quasar X-ray spectra are, however, limited to a dozen or so objects. Within the more than 3000 ROSAT PSPC pointings (covering about 10 % of the sky) lie more than 50,000 sources (White, Giommi & Angelini 1995, Voges et al 1994). Out of these, a sample of several hundred quasar X-ray spectra can be readily compiled for the first time, thanks to the release of the two source catalogs, WGACAT (White, Giommi & Angelini 1995) and ROSATSRC (Voges et al 1994). We have used these data to explore the questions raised by the initial PSPC high redshift quasar studies. As an additional benefit of this program we are able to study the emission spectra of a large sample of radio-loud and radio-quiet quasars and study their differences.

We investigate the connection between low energy X-ray cut-offs and the radio and optical spectra of these quasars in a companion paper (Elvis et al. 1997, Paper II). A later paper (Nicastro et al. 1997) will discuss a sub-sample of quasars selected to have the typical colors produced by absorption features imprinted on the X-ray spectrum by an ionized absorber along the line of sight.

We use a Friedman cosmology with $H_0=50 \text{ km s}^{-1} \text{ Mpc}^{-1}$ and $\Omega = 0$ throughout this paper.

2. The Sample

Quasars were selected by cross-correlating the first revision of the WGA catalog (White, Giommi & Angelini 1995) with a variety of optical and radio catalogs, including the Veron-Cetty & Veron (1993) and Hewitt & Burbidge (1993) quasar catalogs, and the 1 Jy (Stickel et al. 1994) and S4 (Stickel & Kühr 1994) radio catalogs. Uncertain classifications and border line objects have been also checked in the Nasa Extragalactic Database (NED).¹ All the objects selected have optical spectra dominated by nonstellar emission and all show broad emission lines.

The maximum radius adopted for identifying cross-correlation candidates was one arcminute. The resulting distribution of X-ray/optical offsets is shown in Figure 1. The mean offset is $\simeq 18$ arcsec, while the median one is $\simeq 13$ arcsec, in agreement with the estimated errors on the positions of the WGA sources (White et al. 1995). Potential mis-identifications through chance co-incidences were addressed by shifting the X-ray positions by various amounts several times, and repeating the cross-correlations. Using these randomized X-ray positions establishes the chance co-incidence rate to be small. The number of spurious X-ray/optical associations is at maximum 2, i.e. less than 0.5% of the whole sample (see below).

We excluded from the sample:

1. observations of sources with a quality flag in the WGA catalog < 5 (corresponding to problematic detections);

¹The NASA/IPAC Extragalactic Database (NED) is operated by the Jet Propulsion Laboratory, California Institute of Technology, under contract with the National Aeronautics and Space Administration.

2. observations of sources with a signal to noise ratio in the 0.1-2.4 keV energy band less than 7 (to ensure reasonable X-ray color determinations);
3. observations of quasars located at an off-axis angle larger than 45 arcmin, (to avoid large systematic errors due to the uncertainties in the PSPC calibration near the edge of the field of view);
4. fields with a Galactic N_H along the line of sight higher than $6 \times 10^{20} \text{ cm}^{-2}$ (to ensure good low energy signal to noise);
5. quasars with $z < 0.1$ (to eliminate the low luminosity Seyfert galaxies in which absorption is common, e.g. Lawrence & Elvis 1982).

We are then left with 453 quasars for which fluxes in three bands, and so two X-ray colors (“soft” and “hard”), can be derived. This is the largest sample of quasars for which homogeneous X-ray spectral information is available. We used only one observation for each quasar. When more than one observation was available for a quasar we chose the one with the highest signal to noise ratio.

Of these quasars 202 have a radio measurement in the literature, and 167 of those are radio-loud according to the usually adopted definition $R_L = \log(f_r/f_B) > 1$, with f_r radio flux at 5 GHz and f_B the B-band flux (Wilkes & Elvis 1987; Kellermann et al. 1989; Stocke et al. 1992). This translates into a (rest-frame) value of the radio to optical spectral index, $\alpha_{ro} > 0.19$. The sample includes 87 Flat Spectrum Radio Quasars ($\alpha_r < 0.5$), the majority of which are discussed by Padovani et al (1997). Steep Spectrum Radio Quasars account for 62 sources. Note that this flat/steep classification is based mostly on the radio spectrum at only 2 or 3 frequencies. Quasars with complex radio spectra (e.g. GigaHertz Peaked Spectrum (GPS) Sources) could appear in either class. This classification also does not distinguish compact steep spectrum (CSS) radio sources from extended ones. For 18 radio-loud quasars we could find radio measurements at one frequency only, and therefore their radio spectral index is unknown. We assumed $\alpha_R = 0.5$ in calculating α_{ro} . Most of the quasars without radio measurement are likely to be radio-quiet (e.g. Ciliegi et al., 1995) so we include them in the radio-quiet sample, making for 286 radio-quiet quasars in the sample.

In the WGACAT there are another 35 quasars with Galactic $N_H > 6 \times 10^{20}$ but passing all other above points, for which we derive a “hard” color only. Of these 28 are radio-loud.

The redshift distributions for radio-quiet quasars and radio-loud quasars is shown in figure 2. At $z \lesssim 1$ the number of radio-quiet objects is higher than that of radio-loud, due to the higher volume density of radio-quiet quasars. By $z \gtrsim 2$ however, the number of radio-loud

objects is higher than that of the radio-quiet objects, due to the higher L_X/L_{opt} of radio-loud quasars.

3. Effective X-ray Spectral Indices

The WGA catalog provides raw count rates in three energy bands: 0.1-0.4 keV (soft band, S), 0.40-0.86 keV (mid band, M) and 0.87-2 keV (hard band, H) for each entry. The count rates can be combined to form a ‘softness ratio’ (SR=S/M) and a ‘hardness ratio’ (HR=H/M). To allow for the effect of the varying Galactic absorption from source to source these softness and hardness ratios can be converted to ‘effective spectral energy indices’, α_S (0.1-0.8 keV), and α_H (0.4-2.4 keV), assuming the Galactic N_H as derived from 21 cm measurements (Stark et al 1992, Shafer et al, private communication, Heiles & Cleary 1979), “Wisconsin” cross-sections (Morrison & McCammon (1983) and solar abundances (Anders & Ebihara 1982), and using the PSPC calibration.

3.1. Correction for the instrumental point spread function

In converting the three count rates into effective spectral indices, corrections must be applied for the instrumental point spread function (PSF), to take into account the different fraction of counts lost outside the detection region in each energy band. The total PSPC PSF includes two main components: the mirror PSF and the PSPC detector PSF (Hasinger et al 1992a). The mirror PSF is energy independent, and dominates the total PSF at off-axis angles greater than about 20 arcmin. At these large off-axis angles a small detection region loses flux but does not significantly alter the spectral shape.

The detector PSF is, instead, highly energy dependent, and dominates the total PSF at small off-axis angles. Using a small detection region for an off-axis angle < 20 arcmin can strongly alter the spectral shape, predominantly at low energies. (The detector FWHM $\propto E^{-0.5}$). The method used in the WGA catalog to estimate the source count rates uses the counts detected in a box whose size optimizes the signal to noise ratio for each source. For relatively weak sources near the field center, this optimum box size is small, and the number of soft photons lost is greater than that of medium or hard energy photons, giving rise to an artificial reduction of the spectrum at low energies, which in turn can lead to an underestimation of α_S of up to 0.2-0.3.

We corrected the count rates in the three bands for both mirror and PSPC PSF effects. We used the analytical approximations for the energy and off-axis angle dependence of the PSF provided by Hasinger et al (1992b).

This method of estimating spectral indices is similar to the de-reddening procedure used in optical photometry, and is quite robust, with typical systematic uncertainties on α_H smaller than 0.1 (as shown, for example, by Padovani & Giommi 1996 or Ciliegi & Maccacaro 1996). It is particularly suitable for handling large samples of objects (Giommi et al., in preparation) e.g. for the determination of the X-ray spectral index distributions.

However, a systematic uncertainty is present in the spectral indices estimates, because the magnitude of the PSF correction depends on the intrinsic source spectrum. To estimate the magnitude of this uncertainty we calculated five series of α_S and α_H for a grid of assumed source spectra: for the average value for high Galactic latitude line of sight ($N_H = 3 \times 10^{20} \text{ cm}^{-2}$) we used $\alpha_E = 1$, $\alpha_E = 1.5$ and $\alpha_E = 2.5$; for the mean value of energy spectral index ($\alpha_E=1.5$) we used low ($N_H = 10^{20} \text{ cm}^{-2}$) and high ($N_H = 10^{21} \text{ cm}^{-2}$) absorption values. We then calculated the differences between the α_S and α_H calculated for each pair of α_E and N_H and those calculated for $\alpha_E = 1.5$ and $N_H = 3 \times 10^{20} \text{ cm}^{-2}$. The differences in α_H were always smaller than 0.05 and those in α_S were always smaller than 0.15. We therefore use these values as systematic uncertainties in the evaluation of these parameters.

3.2. PSPC background

The WGACAT count rates are not background subtracted. Therefore, another possible source of error in the evaluation of the PSPC spectral indices is the PSPC background in the three WGACAT bands. The PSPC background has been studied in great detail by Snowden et al (1992, 1994, noncosmic background, and 1995, 1997 diffuse, cosmic X-ray background) using ROSAT All Sky Survey (RASS) data and pointed observation data. The energy band which shows, by far, the highest background at high Galactic latitude is the 0.1-0.28 keV range, which spans most of the SOFT band defined in WGACAT (0.1-0.4 keV) We now analyze the effect that a wrong or absent background subtraction in the SOFT band can have on the soft energy index α_S .

The cosmic background in the SOFT band is highly spatially variable, with large regions of maxima of about $0.0015 \text{ counts s}^{-1} \text{ arcmin}^{-2}$ at high Galactic latitudes ($|b| > 30$) and minima of $0.0003 \text{ counts s}^{-1} \text{ arcmin}^{-2}$. Long-Term enhancements are difficult to identify and model in pointed observations. They mainly affect the low frequency part of the spectrum,

$E < 0.28$ keV, where their contribution can even be as high as $0.001 \text{ counts s}^{-1} \text{ arcmin}^{-2}$. We adopt a conservative value for the total SOFT band background of $0.003 \text{ counts s}^{-1} \text{ arcmin}^{-2}$.

The typical box-size of the WGACAT extraction regions is 0.3-0.8 arcmin for off-axis angles smaller than 20 arcmin and 1-3 arcmin for off-axis angles between 20 and 45 arcmin, where the lower limits apply to the faintest sources. Such extraction regions, together with the above background rate would give a few counts in the low energy band in typical exposures of 1000-10000 sec for sources detected in the central 20 arcmin, and a few tens of counts for sources detected in the outer PSPC region.

Let us assume the case of a faint (close to our limit of 7 in signal to noise ratio) and strongly cutoff source, whose counts in the SOFT band are a few, comparable with the background contribution, and 15-30 in the MEDIUM band. In this case the upper limit on the slope between the SOFT and MEDIUM energy bands differs from the slope we would measure neglecting background subtraction by ~ 0.5 . This compares with a typical statistical error in α_S of 0.5-0.7 for such faint sources and with a systematic uncertainty of 0.15. We conclude that the small extraction regions used in the WGACAT means that background is not a significant problem, even for the SOFT band count rate of our faint sources. As a result we did not subtract background in the evaluation of the effective spectral indices α_S and α_H .

To investigate the robustness of this assumption, we searched for correlations between the soft and hard effective spectral indices and (1) the size of the extraction region, (2) the off-axis angle, and (3) the source count rate. Any correlations would be evidence that neglecting the background was causing problems. In no case did we find significant correlations. We conclude that neglecting the background subtraction does not strongly affect or bias our results.

There are other two sources of uncertainties in the spectral indices estimates: first, quasars located near the PSPC rib structures can suffer a preferential loss of soft photons. We inspected the original ROSAT images for each source that appeared to have unusually low soft band counts and rejected those that might have been so affected. Second, the spectral indices estimates from hardness ratios may be significantly different from the results of a proper spectral fit to the full PHA spectrum, in presence of a curvature in the intrinsic spectrum, because of the skewness induced in the broad energy bands used to construct the hardness ratios. For all these reasons the effective spectral indices α_S and α_H should not be regarded as a measure of the true emission spectral indices. They should rather be regarded as a rough estimation of the “average” soft and hard spectral shapes. They are the soft X-ray analogs of (U-B), (B-V) colors, for which multiple physical interpretations are possible. We will use α_S as an indicator of a possible low energy cut-off.

3.3. Effective Spectral Indices and Quasar Properties

The radio-quiet and radio-loud quasars α_S and α_H are plotted against each other in figure 3a,b. In the radio-loud plot flat spectrum radio sources are identified by circles, and steep spectrum sources by squares. High redshift quasars ($z > 2.2$) are shown with filled symbols. The range of α_S and α_H are large and so the different parts of the diagram correspond to radically different spectral shapes. These are illustrated with three-point spectra in figure 3. For the purpose of this paper we are most interested in those for which a low energy cut-off is indicated (lower center of figure 3).

To study these features more closely we divided the quasars into four redshift bins: 0.1-0.5; 0.5-1; 1-2.2; and $z > 2.2$. Table 1 gives the average spectral indices (α_S, α_H) and their dispersions ($\sigma(\alpha_S), \sigma(\alpha_H)$) in these four redshift bins for both radio-quiet and radio-loud quasars. The typical statistical uncertainties on α_S and α_H are ± 0.2 , the systematic uncertainty is at most ± 0.15 for α_S and ± 0.05 for α_H , so the measured dispersions are not strongly affected by these uncertainties.

3.3.1. Radio-Loud vs. Radio-Quiet

The mean and dispersion of α_H and α_S for the radio-quiet quasars are (1.59, 0.52) and (1.69, 0.41); those of radio-loud quasars are (1.13, 0.55) and (1.32, 0.59). The difference of ~ 0.5 in α_H agrees with the widespread finding that radio-loud quasars have flatter X-ray spectra than radio-quiet quasars (e.g. Elvis & Wilkes 1987, Laor et al., 1994, Laor et al., 1997, Schartel et al., 1996a).

For radio-quiet quasars the distribution of α_S is consistent with that of α_H in all redshift bins. In the last redshift bin there are only 12 quasars (see Table 1), and only three at $z > 2.5$, and therefore the test is not very stringent for this redshift interval. This uniformity suggests a single emission mechanism dominating the whole ROSAT band (c.f. Laor et al., 1997), at least for redshifts smaller than about 2.

Radio-loud quasars, instead, have α_H smaller than α_S by ~ 0.2 (i.e. a concave spectrum) in the low redshift bins ($z < 2.2$). The Kolmogorov-Smirnov probability of α_S being drawn from the same distribution function as α_H , is 5.0 % for redshifts 0.1–0.5, 22 % for redshifts 0.5–1.0 and 0.14 % for redshifts 1.0–2.2. This new result could be interpreted in terms of an additional component in the spectrum of radio-loud quasars above that seen in radio-quiet quasars (as suggested earlier by e.g. Wilkes & Elvis 1987). However, it may also imply

Table 1: **Quasars Average Spectral Indices & Cut-off statistics**

z bin	N	α_S	$\sigma(\alpha_S)$	N	α_H	$\sigma(\alpha_H)$	no. cut-off	fraction
Radio-Quiet Quasars								
0.1–0.5	136	1.73	0.48	141	1.62	0.51	7	0.051
0.5–1.0	66	1.68	0.36	67	1.67	0.51	3	0.045
1.0–2.2	72	1.67	0.38	72	1.51	0.49	1	0.014
>2.2	12	1.54	0.26	13	1.32	0.69	0	0
Radio-Loud Quasars								
0.1–0.5	34	1.49	0.52	41	1.20	0.63	1	0.029
0.5–1.0	45	1.30	0.62	51	1.18	0.48	2	0.044
1.0–2.2	70	1.37	0.52	78	1.13	0.51	4	0.057
>2.2	18	0.89	0.71	25	0.89	0.60	7	0.389
Flat Spectrum Radio Quasars								
0.1–0.5	9	1.38	0.30	14	1.32	0.38		
0.5–1.0	26	1.24	0.73	30	1.11	0.51		
1.0–2.2	40	1.35	0.50	43	0.99	0.46		
>2.2	12	0.74	0.75	17	0.78	0.60		
>0.1	87	1.24	0.63	104	1.04	0.51		
Steep Spectrum Radio Quasars								
0.1–0.5	19	1.52	0.62	21	0.96	0.65		
0.5–1.0	14	1.29	0.44	16	1.23	0.39		
1.0–2.2	24	1.40	0.58	28	1.12	0.46		
>2.2	5	1.15	0.58	7	1.33	0.60		
>0.1	62	1.37	0.56	72	1.14	0.56		

different processes at work in radio-loud and radio-quiet quasars, (as also suggested by Laor et al., 1997). To disentangle these two possibilities a careful analysis of the optical to X-ray Spectral Energy Distribution of WGACAT quasars is needed. This is beyond the scope of this paper and will be addressed in a forthcoming paper.

We have computed the mean α_S and α_H for the two samples of flat and steep radio spectrum quasars. These are reported in Table 1. Although both distributions of α_S and α_H for the steep and flat radio quasars are consistent with being drawn from the same distribution function (using a K-S test), the mean α_S of steep radio spectrum quasars is steeper than that of flat radio spectrum quasars (at the 90 % confidence level). The mean α_H of the two samples of quasars is on the other hand very similar. Redshift bins 0.1-0.5 and $z > 2.2$ are populated by too small a number of flat radio spectrum and steep radio spectrum quasars respectively to allow a statistically significant comparison. In the other two redshift

bins the distributions of α_H and α_S of the two samples are consistent with each other.

The dispersion in α_H and α_S is large for both radio-quiet and radio-loud quasars. The radio-loud dispersion in α_S is larger than that of radio-quiet quasar at a confidence level of 96 %. Emission or absorption mechanisms that produce more varied outputs seems to be needed for radio-loud quasars.

From figure 3 it appears that the number of radio-loud quasars with $\alpha_S < 0.5$ is much larger than the number of radio-quiet with $\alpha_S < 0.5$, especially at high z (solid symbols). This is the sense of the change in α_S to produce low energy cut-offs, as would be produced by photoelectric absorption.

We compare the distribution of radio-loud and radio-quiet indices about their respective mean α_S (figure 4). By offsetting from the mean of each group we remove the difference in the group means discussed above. Figure 4 shows the broader dispersion of α_S for radio-loud quasars. It also shows a population of radio-loud quasars with smaller α_S , i.e. quasars that show low energy cut-offs. This tells us with high confidence that the cut-offs are not due to intervening material. Intervening material would not ‘know’ whether a background quasar was radio-loud or radio-quiet. The cause of the cut-offs must be physically associated with the quasar in some way.

3.3.2. *Dependence on Redshift*

To quantify the differences with redshift and study their evolution we plot α_H and α_S versus redshift for radio-quiet and radio-loud quasars in figures 5a,b and 6a,b respectively. There is no strong evidence of evolution of either α_H or α_S with redshift for radio-quiet quasars. Again the small number of radio-quiet quasars with $z > 2$ does not allow us a strong conclusion to be drawn for high redshift objects. For the bins $0.5 < z < 1$ and $1 < z < 2.2$ the probability that the two distributions of α_H are drawn from the same distribution function is marginally unacceptable (P=4.5%), in agreement with previous studies (Schartel et al 1996b).

On the other hand radio-loud quasars show strong changes in both α_S and α_H for $z > 2.2$, in the sense that both indices are smaller than in lower redshift bins. We ran a Kolmogorov-Smirnov test between the distributions of spectral indices in each possible pair formed with the four redshift bins. The distributions of α_S and α_H at $z < 2.2$ are all consistent with each other. Only the $z > 2.2$ bin shows significant differences from the others, for both

α_S and α_H . Table 2 gives the percentage probability that the spectral index distributions of α_S and α_H in two redshift bins are drawn from the same distribution function.

Table 2: Kolmogorov-Smirnov test for Radio Loud Quasars

α_S				
	0.1–0.5	0.5–1.0	1.0–2.2	> 2.2
>2.2	3.0	5.8	2.1	–
α_H				
>2.2	0.10	4.1	0.16	–

Some caution is required however. In flux limited samples redshift and luminosity are often degenerate, so that it is hard to distinguish the effects of one from the other. The apparent trend with redshift discussed above may thus be induced by a correlation with luminosity (figure 7a). We tested for this degeneracy by selecting a sub-sample of only the high $\log(L_{opt})$ (>32) quasars. The correlation between α_S and z for this sample is still very good (figure 7b, linear correlation coefficient $r = -0.46$, which, for 43 points, corresponds to a probability of 99.8%). On the other hand, the correlation between α_H and z for the high luminosity, high redshift quasar is not significant, $r = -0.17$ (probability of 72%).

To better disentangle the luminosity/redshift dependence of α_S and α_H we also performed a partial correlation analysis (e.g., Kendall & Stuart 1979) on the whole radio-loud sample. While α_S is anti-correlated with redshift even subtracting the effect of the optical luminosity ($P \simeq 99.9\%$), in the case of α_H no correlation with redshift is left once the luminosity dependence is subtracted out ($\simeq 48\%$). On the other hand, excluding the redshift dependence, we find that α_H is anti-correlated with luminosity at the 99.2% level.

We conclude that the flat α_S , unlike α_H , are truly more common at high redshifts, and so are an evolutionary, or cosmological, effect.

3.3.3. Low Energy Cut-offs

The high incidence of low energy cut-offs at high redshifts can be made clearer by defining a sample of ‘candidate cut-off’ objects using α_S and then examining the fraction that occur among both radio-loud and radio-quiet quasars as a function of redshift.

The change in index of radio-loud quasars can be seen in figure 6b as due to a population of radio-loud quasars with a soft spectral index significantly smaller than the average and

smaller than the hard spectral index. (Although there are also a few radio-quiet quasars with exceptionally flat α_S , figure 5b). These small α_S quasars are ‘cut off’ in their low energy spectrum compared with an extrapolation of the hard spectrum.

We select ‘candidate’ low energy cut-off quasars using three criteria. (1) $\alpha_S < \alpha_H$; (2) $\alpha_S < 0.5$ selects all the high redshift radio-loud candidates apparent in figure 6b. (3) Lower redshift radio-loud and all radio-quiet candidates require a more careful selection since their mean α_S are different. We use the criterion that they have α_S smaller than the average by at least 0.75. For radio loud quasars the average α_S at $z < 2.2$ is 1.32 and therefore we selected quasars with $\alpha_S < 0.58$ in this redshift interval. For radio-quiet quasars there is no evidence for a change in the average α_S with z and therefore we selected the quasars with $\alpha_S < 0.94$ (the average α_S is 1.69). These criteria select 10 radio-quiet and 14 radio-loud ‘candidate’ cut-off quasars. Table 3 gives the optical or radio names, redshift and optical luminosity of these objects.

The distribution of ‘candidate’ cut-offs is striking. Table 1 gives the total number of quasars, the number of “candidate” cut-off quasars and its fraction in each redshift bin, while figure 8 shows the fraction of ‘candidate’ cut-off quasars as a function of z for both quasar samples. The fraction of “candidate” cut-off quasars among the 18 radio-loud objects at $z > 2.2$ is significantly different from that at $z < 2.2$ (probability of 0.002 %, using the binomial distribution). For radio-quiet objects the absence of cut-offs among the 12 quasars at $z > 2.2$ is consistent with the cut-offs distribution at lower redshift (probability of 50 %). In turn, the probability of finding zero ‘candidate’ cut-off quasars among the $n=12$ radio quiet quasars at $z > 2.2$, assuming a frequency of cut-offs similar to that of radio loud quasars at the same redshift, is 0.3 %.

This strongly suggests a difference in the ‘candidate’ cut-off quasar distribution with z between radio loud and radio quiet objects. We calculated, using the Fisher exact probability test (e.g. Siegel 1956), the probability that the two “candidate” cut-off samples differ in the proportion with which they are distributed in redshift, e.g. below and above a given redshift. For $z=2.2$ the difference is significant at the 98.4% level.

4. X-ray Spectra

A flatter α_S at high redshift than at low redshift can be due to at least three effects: (a) the redshifting of a soft component contributing at the emission below $\approx 1 - 3$ keV (quasar frame) out of the observed energy range for $z \gtrsim 2$; (b) evolution of the emission spectrum;

(c) a cut-off due to low energy absorption becoming more frequent at $z \gtrsim 2$. A simple color analysis cannot distinguish between these three possibilities. A two parameter spectral fit can discriminate more strongly, and is possible for the quasars with a few hundreds detected PSPC counts. This section investigates such fits.

Most of the quasars in the sample do not have published PSPC spectral fits. We extracted the full pulse height spectrum for each of the quasars in the sample from the appropriate event files in the ROSAT archive. We used standard extraction criteria (see e.g. Fiore et al. 1994, Elvis et al 1994a). Table 4 gives the total counts in the 0.1-2.4 keV energy band, the exposure and the off-axis angle for these quasars. All the radio-loud quasars were observed on-axis and were the target of their observation. All the radio-quiet quasars (except RXJ16331+4157) are instead serendipitous sources in ROSAT fields. With one exception (SBS0945+495) the radio-quiet quasars all lay within the inner PSPC rib ($r = 18$ arcmin), where the calibration is most accurate.

We then fitted the spectra with a power law model with low energy absorption (at $z=0$). We made four fits for each quasar: We first let the column density be free to vary, and then kept it fixed to the Galactic (21 cm) value along the line of sight. Similarly, we let the power law spectral index be free to vary, and then kept it fixed to the mean value of α_H at the redshift of the quasar (Table 1). The results are given in Tables 5 and 6 for each quasar sample. Listed are: the best fit parameters, the χ^2 , and the probability that the improvement in χ^2 between the fits with free N_H and N_H fixed to the Galactic value is significant (calculated using the χ^2 distribution with 1 dof for the $\Delta\chi^2$).

From Tables 5,6 we see that the evidence of a cut-off is very robust (‘Class A’) for four radio-loud quasars (PKS2126–158, PKS0438–436, 3C 212, and 3C 207), Probability $\gtrsim 99.9\%$. For another four radio-loud quasars (S4 1745+624, PKS2351–154, S4 0917+449 and PKS1334–127) the probability of a cut-off is $\gtrsim 95\%$ (‘Class B’). For S4 0917+624 the probability for a cut-off is $\gtrsim 92\%$ (‘Class C’). Furthermore three quasars (3C219, PKS0537-286 and S4 0636+680) have very flat energy index, much flatter than the average for radio loud quasars at those redshifts, if we insist on only Galactic absorption (we also call these ‘Class C’). Excess absorption, similar to that required in the better spectra, readily produces a normal energy index. Two radio-loud quasars do not show any evidence for a cut-off (4C71.07 and PKS1442+101). The first is a famous blazar, detected by EGRET in the GeV energies (e.g. von Montigny et al 1995) and therefore beaming is important. The second is often classified as a Compact Steep Radio Spectrum quasar (e.g. DallaCasa et al 1995). The total number of cut-off radio loud quasars is therefore eight, with three more objects likely to be cut-off quasars.

By contrast, in radio-quiet quasars we have a strong evidence for a cut-off in only one case out of 289 (PHL6625, Probability $> 99.9\%$). PHL6625 lies just 4.6 arcmin from the position of the low redshift galaxy NGC 247. The cut-off in PHL6625 may well be due to absorption in gas associated to NGC247 (Elvis et al., 1997). Two other radio quiet quasars MS03363-2546, US3333) have a probability for a cut-off $\gtrsim 95\%$. US3333 is included in the area of the sky already surveyed by the NVSS (Condon et al., in preparation) but has not been detected. The upper limit on the radio flux ($f_r < 2.5$ mJy) puts an upper limit of 0.2 on α_{ro} , very close to the threshold of 0.19 that we use to divide radio-loud and radio-quiet quasars. More sensitive optical and radio observation are then needed to assess the nature of this source. MS03363-2546 is not detected in radio by Stocke et al 1992. The limit on the radio flux assures that this quasar is a truly radio-quiet source. The origin of the cut-offs of MS03363-2546 and US3333 is unknown and deserves follow-up studies. The probability of finding by chance the detected number of cut-off radio quiet quasar at $z < 2.2$, assuming a frequency of cut-offs similar to that of radio loud quasars is 1.3 %.

5. Comparison with previous results

Results on the ROSAT pointed observations of the quasars in Table 3 have been published by Elvis et al (1994a, PKS0438-436, PKS2126-158, S40636+680), Elvis et al (1994b 3C212), Maraschi et al (1995, PKS1334-127), Brunner et al (1994, 4C71.07), Buhler et al. (PKS0537-286), Bechtold et al. (1994, PKS1442+101 and S41745+624).

The spectral fitting results in Table 6 generally agree well with the results presented in the above papers. Maraschi et al (1995) use a Galactic N_H higher than the one we adopted (from Stark et al 1992) by about $1.6 \times 10^{20} \text{ cm}^{-2}$, and as a result conclude that there is little evidence for absorption in this source.

Some of the quasars in Table 3 have also been observed by ASCA (Siebert et al., 1996 PKS0537-286, Cappi et al., 1997, PKS0438-436, PKS0537-286, 4C71.07, PKS2126-158). The results found by these authors are consistent with those obtained from the ROSAT observations with the exception of 4C71.07, for which Cappi et al. (1997) report significant intrinsic absorption (of about $8 \times 10^{20} \text{ cm}^{-2}$). The comparison between the ROSAT and the ASCA data implies a variation in the absorber column density on a time-scale of less than 2.6 years in this source. Cappi et al. (1997) discuss in detail the possibility that low energy absorption in addition to the 21 cm value in their sample of high redshift quasars may be due to molecular gas. For the four quasars in common between their and our sample they find no strong evidence for Galactic molecular gas absorption. We note here that our limit on

the Galactic (21cm) N_H effectively excludes low Galactic latitude sources from our sample, thus minimizing the probability for a contamination from Galactic molecular clouds, which are strongly concentrated toward the Galactic plane. The CO survey by Blitz, Magnani & Mundy (1984) finds that molecular gas is uncommon at high Galactic latitudes. The only quasar known to be affected by molecular gas absorption (NRAO140, Marscher 1988, Turner et al., 1995) lies at low Galactic latitude, and was excluded from our sample because it has a Galactic (21 cm) N_H of $1.4 \times 10^{21} \text{ cm}^{-2}$. Furthermore, de Vries, Heithausen & Thaddeus (1987) found that high Galactic latitude molecular clouds differ from the Galactic plane clouds so that their CO-to-H₂ conversion factor is significantly smaller: $\sim 0.5 \times 1020$ instead of $\sim 2 - 4 \times 1020 \text{ molecules cm}^{-2} (\text{K}^{-1} \text{ km}^{-1} \text{ s})^{-1}$ (Combes, 1991). This would reduce the additional hydrogen column density implied by any CO emission by a factor ~ 6 .

The evolution of the quasar X-ray spectrum has also been studied by three groups: Schartel et al (1996a) who used a sample drawn from the RASS containing all quasars with $M_V < -23$ and more than 80 RASS counts; Schartel et al (1996b) used the Large Bright Quasar Sample (LBQS) quasars observed during the RASS (using both detections and non-detections); Puchnarewicz et al (1996) used AGNs identified in the ROSAT International X-ray/Optical Survey (RIXOS).

All the radio-quiet objects in Schartel et al (1996a) are at $z < 0.5$, while radio-loud objects are detected up to $z=2.5$. The indices of the radio-quiet objects are fully consistent with those of the WGACAT quasars. The PSPC spectral indices of radio-loud objects show a significant flattening above $z \sim 1$, which is interpreted by Schartel et al in terms of a selection effect and/or a redshift effect, if quasar spectra are not simple power laws (but rather have a concave shape). In the WGACAT quasars we see little change in both α_S and α_H from $0.1 < z < 2$, most of the evolution being confined at redshifts higher than ~ 2 .

On the other hand most of the LBQS objects studied by Schartel et al (1996b) are radio-quiet quasars. Schartel et al (1996b) find a marginal (2 sigma) evidence for a flattening of LBQS spectra at $z \gtrsim 1.5$. This result is consistent with our findings (see Section 3.1.2 above) based on WGACAT quasars. In particular the slopes reported by Schartel et al (1996b) agree well with those in Table 1. Again, the study of the evolution of the spectrum of radio-quiet quasars is limited by the fact that high redshift radio-quiet quasars are faint and not easy to observe with ROSAT.

Puchnarewicz et al (1996) find a mean energy index significant flatter than those obtained from the WGACAT quasars. They also find no evidence for a change in α_X with z . The flat average slope reported by Puchnarewicz et al could be due to the selection criteria used to define the sample (a flux limit of $3 \times 10^{-14} \text{ erg cm}^{-2} \text{ s}^{-1}$ in the ROSAT 0.4-2 keV ‘hard band’) which favors the inclusion in the sample of flatter AGN. Furthermore, the

correlation between the optical to X-ray index with the X-ray spectral index (like the one found in Seyfert galaxies and low redshift quasars, see eg. Walter & Fink 1993, Fiore et al. 1995) can select preferentially flat X-ray quasars when considering a strictly X-ray selected sample (low optical to X-ray index). We also note (from their figure 3) that in their sample there are a few quasars with a very flat spectral index, possibly due to absorption, which tend to lower the average index. These quasars have a red optical continuum, strengthening the evidence for absorption in these cases.

Also the fraction of radio-loud AGN in the RIXOS is unknown. The energy index Puchnarewicz et al (1996) find at $2 < z < 3$ is similar to the index we find in the same redshift interval for radio-loud objects. At low redshift the radio quiet population should dominate in number (because of its much larger volume density). However, we note that a similar X-ray flux limited survey (Schartel et al 1996a) is completely dominated by radio loud objects at $z \gtrsim 0.5$, since radio-loud objects are brighter in X-rays than radio quiet (e.g Zamorani et al 1981, Green et al 1996). Therefore the RIXOS indices, at least at high redshift, could be dominated by the radio-loud population.

6. Conclusions

We have studied the 2 color X-ray spectra of a sample of about 167 radio-loud quasars and 286 ‘bona fide’ radio-quiet quasars. Radio-loud quasars cover the whole redshift space from 0.1 to 4 rather uniformly, while there are only three radio-quiet quasars at $z > 2.5$, against 12 radio-loud quasars at the same redshifts. Any conclusion on radio-quiet quasars then apply to $z \lesssim 2$ only.

Concerning the low energy cut-off we have established:

1. Low energy X-ray cut-offs are more commonly (and perhaps exclusively) associated with radio-loud quasars. Detailed spectral fits allow us to add, with some confidence, that photoelectric absorption is a likely origin of the ‘low energy cut-offs’. The conclusion is that *low energy X-ray cut-offs are associated with the quasars*, and not with intervening systems, since those would affect radio-quiet and radio-loud quasars equally.
2. Among radio-loud quasars those at high redshift have a lower mean α_S than those at low z (P=0.04%), with many lying in the X-ray ‘cut-off’ zone. Detailed spectral analysis of all candidate cut-off quasars show four robust cut-off detections at redshift higher than 2.2. The probability that the fraction of cut-off quasars among the 18

objects at $z > 2.2$ is similar to that of radio-loud quasars at $z < 2.2$ is very small, about 0.002 % (using the binomial distribution). This indicates that cut-offs were more common in the past than they are now. I.e. *the X-ray cut-offs show evolution with cosmic epoch.*

3. The degeneracy between redshift and luminosity found in flux limited samples of quasars was tested by using a partial correlation analysis. We found that while α_S is truly anti-correlated with redshift at the 99.9% confidence level, in the case of α_H the observed anti-correlation with redshift is mostly due to a strong dependence on luminosity. Therefore, the cut-offs are an evolutionary, not a luminosity, effect.

Concerning the emitted X-ray spectra of quasars we have established:

4. The distribution of α_S of radio-quiet quasars is consistent with that of α_H for $z \lesssim 2$. This uniformity suggests a single emission mechanism dominating the whole ROSAT band (c.f. Laor et al., 1997) up to a redshift of about 2. We find a marginal evidence for a flattening of α_H (P=4.5 %) going from $z < 1$ to $z = 2$, in agreement with previous studies (Schartel et al 1996b). This can be due to a selection effect even if quasar X-ray spectra are simple power laws, because at high redshift the steepest (and therefore faintest) sources would not be detected. However, it is well known that ROSAT PSPC 0.1-2 keV spectral indices of Seyfert 1 galaxies and low redshift radio-quiet quasars are much steeper than those observed above 2 keV (e.g. Walter & Fink 1993, Fiore et al 1994, Laor et al 1997). If the spectrum of these AGN is made up of two distinct components that are equal at a typical energy E_0 , the flattening of α_H at $z > 1$ would suggest that E_0 lies in the range 2-4 keV (quasar frame).
5. Radio-loud quasars at $z < 2.2$ show a ‘concave’ spectrum ($\alpha_H < \alpha_S$ by ~ 0.2). Both indices are much flatter than those of radio-quiet quasars. This new result is in line with the suggestion of Wilkes & Elvis (1987) that the X-ray spectrum of radio-loud quasars may be due to an additional component above that seen in radio-quiet quasars. However, it may also imply different processes at work in radio-loud and radio-quiet sources (as recently suggested by Laor et al., 1997).

At $z \gtrsim 2$ the average soft and hard indices are similar and both significantly smaller than at lower redshifts. This could be due to the soft component of radio-loud quasars being completely shifted out of the PSPC band at $z > 2$. Most $z > 2$ radio-loud quasars in our sample have flat radio spectra. Padovani et al. (1997) suggested that these quasars are analogs to LBL BL Lacs, that is BL Lac objects with maximum energy emission in the IR-Optical band. Their high energy radiation should then be dominated by inverse Compton emission. At $z > 2$ we are then likely seeing pure inverse Compton

emission. At lower redshift the ROSAT PSPC band could sample a mixture of inverse Compton emission, the tail of the Synchrotron component peaking in the infrared and thermal emission from the hypothesized accretion disk.

The radio and optical properties of the quasars with low energy X-ray cut-offs will be discussed in more detail in a companion paper (Elvis et al. 1997).

This research has made use of the BROWSE program developed by the ESA/EXOSAT Observatory, NASA/HEASARC, and the NASA/IPAC Extragalactic Database (NED) which is operated by the Jet Propulsion Laboratory, California Institute of Technology, under contract with the National Aeronautics and Space Administration.

REFERENCES

- Anders, E., Ebihara, M. 1982, *Geochim. Cosmochim. Acta*, 46, 2363
- Bechtold, J., Elvis, M., Fiore, F., Kuhn, O., Cutri, R.M., McDowell, J.C., Rieke, M., Siemiginowska, A., Wilkes, B.J. 1994, *AJ*, 108, 374
- Blitz, L., Magnani, K., Mundy, L. 1984, *ApJL*, 282, L9
- Brunner, H., Lamer, G., Worrall, D.M., Staubert, R. 1994, *A&A*, 287, 436
- Buhler, P., Courvoisier, T.J.-L., Staubert, R., Brunner, H., Lamer, G. 1995, *A&A* 295, 309
- Cappi, M. et al. 1997, *ApJ*, in press
- Ciliegi, P., Maccacaro, T. 1996, *MNRAS*, 282, 477
- Combes, F. 1991, *ARAA*, 29, 195
- Dalla Casa, D., Fanti, C., Schilizzi, R.T., Spencer, R.E. 1995, *A&A*, 295, 27
- de Vries, H.W. Heithausen, A., Thaddeus, P. 1987, *ApJ* 319 723
- Elvis, M., Lawrence, A. 1985, in "Astrophysics of Active Galaxies and Quasi-Stellar Objects", ed. J.Miller [Univ.Science Press: Mill Valley CA]
- Elvis, M., Fiore, F., Wilkes, B.J., McDowell, J., Bechtold, J. 1994a, *ApJ*, 422, 60
- Elvis, M., Fiore, F., Mathur, S., Wilkes, B. 1994b, *ApJ*, 425, 103
- Elvis, M., Mathur, S., Wilkes, B. 1995, *ApJ*, 452, 230
- Elvis, M., Fiore, F., Giommi, P., Padovani, P. 1997, *ApJ*, in preparation (Paper II)
- Fiore, F., Elvis, M., McDowell, J. C., Siemiginowska, A., Wilkes, B.J., 1994, *ApJ*, 431, 515

- Fiore, F., Elvis, M., Siemiginowska, A., Wilkes, B.J., McDowell, J.C., Mathur, S. 1995, ApJ, 449, 74
- Giommi, P. et al. 1997, in preparation
- Green, P.J., et al. 1995, ApJ, 450, 51
- Hasinger, G. et al 1992, Legacy, 2, 77, OGIP MEMO, CAL/ROS/92-001
- Heiles C. and Cleary M.N., 1979, Aust. J. Phys. Suppl., 47, 1
- Hewitt, A., Burbidge, G. 1993, ApJS, 87, 451
- Hill, G.J., Goodrich, R.W., DePoy, D.L., 1996, ApJ, 462, 163
- Kellermann, K. I., Sramek, R., Schmidt, M., Shaffer, D. B., Green, R. 1989, AJ, 98, 1195
- Kendall, M., Stuart, A. 1979, The Advanced Theory of Statistics, MacMillan, New York
- Lawrence, A., Elvis, M. 1982, ApJ, 256 410
- Laor, A, Fiore, F. Elvis, M., Wilkes, B.J. McDowell, J.C.M. 1997, ApJ, 477, 93
- Laor, A, Fiore, F. Elvis, M., Wilkes, B.J. McDowell, J.C.M. 1994, ApJ, 435, 611
- Maraschi, L., Fossati, G., Tagliaferri, G., Treves, A. 1995, ApJ, 443, 478
- Marscher 1988, ApJ, 334, 552
- Morrison, R., McCammon, D. 1983, ApJ, 270, 119
- Nicastro, F. et al. 1997, ApJ, in preparation
- Padovani P., Giommi P. 1996, MNRAS, 279, 526
- Padovani, P., Giommi, P., Fiore, F. 1997, MNRAS, 284, 569
- Pfefferman, E., et al 1987, Proc SPIE, 733, 519
- Puchnarewicz, E.M. et al. 1996, MNRAS, 281, 1243
- Schartel, N., Walter, R. Fink, H.H., Trümper, J. 1996a, A&A, 307, 33
- Schartel, N., et al. 1996b, MNRAS, 283, 101
- Siebert, J., Matsuoka, M., Brinkmann, W., Cappi, M., Mihara, T. Takahashi, T., 1996, A&A, 307, 8
- Siegel, S. 1956 ‘Non Parametric Statistics’, New York: McGraw-Hill
- Snowden, S.L., Plucinsky, P.P., Briel, U., Hasinger, G., Pfefferman, E. 1992, ApJ, 393, 819
- Snowden, S.L., McCammon, D., Burrows, D.N., Mendenhall. J.A. 1994, ApJ, 424 714
- Snowden, S.L., Freyberg, M.J., Schmitt, J.H.M.M., Voges, W., Trümper, J., Edgar, R.J., McCammon, D., Plucinsky, P.P., Sanders, W.T. 1995, ApJ, 454, 643

- Snowden, S.L., Egger, R., Freyberg, M.J., McCammon, D., Plucinsky, P.P., Sanders, W.T., Schmitt, J.H.M.M., Trümper, J., Voges, W. 1997, ApJ, 485, in press
- Stark, A. A., Gammie, C. F., Wilson, R. W., Bally, J., Linke, R. A., Heiles, C., Hurwitz, M., 1992, ApJS, 77
- Stickel, M., Kühr, H., 1994, A&AS, 103, 349
- Stickel, M., Meisenheimer, K., Kühr, H., 1994, A&AS, 105, 211
- Stoeckle, J. T., Morris, S. L., Weymann, R. J., Foltz, C. B. 1992, ApJ, 396, 487
- Trümper, J. 1983, Adv. Space Res., 2, No. 4, 241
- Turner, T.J. et al. 1995, ApJ, 445, 660
- Véron-Cetty, M.-P., Véron, P., 1993, A Catalogue of Quasars and Active Nuclei, 6th ed. ESO Scientific Report No. 13
- von Montigny, C. et al. 1995, ApJ, 440, 525
- Walter, R., Fink, H.H. 1993, A&A, 274, 105
- Wilkes, B.J., Elvis, M. 1987, ApJ, 323, 243
- Wilkes B.J., Elvis M., Fiore F., McDowell J.C., Tananbaum H. Lawrence A. 1992, ApJL, 393, L1
- White, N. E., Giommi, P., Angelini, L., 1995,
<http://lheawww.gsfc.nasa.gov/users/white/wgacat/wgacat.html>
- Zamorani, G. et al, 1981, ApJ, 245, 357

Table 3: ‘Candidate’ Cut-off Quasars

Quasar	z	$\log L_O$ erg s^{-1}
Radio Quiet		
RXJ16331+4157	0.136	29.14
MS02388-2314	0.284	29.92
Q0335-350	0.321	29.68
MS03363-2546	0.334	30.20
US3333	0.354	30.55
PHL6625 ^a .	0.38	29.98
MS12186+7522	0.645	30.77
Q1234+1217	0.664	30.67
MS21340+0018	0.805	30.31
SBS0954+495	1.687	31.32
Radio Loud		
3C219	0.174	29.93
PKS1334-127	0.539	31.08
3C207	0.684	30.98
3C212	1.043	30.91
S4 0917+624	1.446	31.29
S4 0917+449	2.18	32.01
4C71.07 ^b	2.19	33.04
PKS2351-154	2.665	32.33
PKS0438-43	2.852	32.46
PKS0537-286	3.119	32.16
S4 0636+680	3.174	33.04
PKS2126-158	3.266	33.25
PKS1442+101	3.53	32.7
S41745+624	3.886	32.97

a. 4.6’ from NGC247 nucleus

b. Blazar, EGRET γ -ray

Table 4: “Candidate” Cut-off Quasars: PSPC Observations

Quasar	Counts	exposure sec	off-axis angle arcmin
Radio Quiet			
RXJ16331+4157	281	13636	on
MS02388-2314	223	8008	16.4
Q0335-350	744	17957	13.0
MS03363-2546	938	50058	18.7
US3333	416	11863	13.2
PHL6625	328	19072	3.0
MS12186+7522	321	6484	14.6
Q1234+1217	114	9426	13.5
MS21340+0018	86	5201	11.6
SBS0954+495	182	3669	35
Radio Loud			
3C219	509	4386	on
PKS1334-127	516	3614	on
3C207	452	7017	on
3C212	770	21565	on
S4 0917+624	366	19465	on
S4 0917+449	640	3367	on
4C71.07	5254	6993	on
PKS2351-154	419	6335	on
PKS0438-43	163	21231	on
PKS0537-286	555	9487	on
S40636+680	68	5342	on
PKS2126-158	1262	7392	on
PKS1442+101	655	15433	on
S41745+624	506	16141	on

Table 5: “Candidate” Cut-off Radio Quiet Quasars: Spectral Fits

Quasar	N_{HGal} 10^{20} cm^{-2}	N_H 10^{20} cm^{-2}	α_E	χ^2/dof	prob. ($\Delta\chi^2$)
Radio Quiet					
RXJ16331+4157	1.05	$1.1^{+2.1}_{-1.1}$	$0.87^{+0.80}_{-0.60}$	7.0/13	
		$2.7^{+0.8}_{-0.4}$	1.6 FIXED	9.2/14	–
MS02388-2314	2.29	$5.5^{+7.3}_{-3.1}$	1.0 ± 0.8	4.8/14	
		2.29 FIXED	0.32 ± 0.25	5.9/15	–
		$8.2^{+3.8}_{-3.0}$	1.6 FIXED	5.9/15	–
Q0335-350	1.26	$2.1^{+1.0}_{-0.8}$	1.18 ± 0.35	14.8/23	
		1.26 FIXED	0.86 ± 0.08	17.2/24	–
		3.1 ± 0.3	1.6 FIXED	17.6/24	–
MS03363-2546	1.05	$2.1^{+1.8}_{-0.8}$	1.28 ± 0.30	72.6/67	
		1.05 FIXED	0.89 ± 0.06	77.4/68	97.2 %
		2.9 ± 0.2	1.6 FIXED	74.3/68	
US3333	4.36	$7.7^{+5.1}_{-2.5}$	1.36 ± 0.55	8.2/15	
		4.36 FIXED	0.77 ± 0.14	12.8/16	96.8 %
		9.0 ± 0.2	1.6 FIXED	8.7/16	–
PHL6625	1.47	$7.7^{+3.0}_{-2.8}$	1.88 ± 0.6	2.5/12	
		1.47 FIXED	0.32 ± 0.14	19.3/12	99.995 %
MS12186+7522	3.02	3.0 FIXED	0.7 ± 0.5	5.7/11	
		$6.5^{+1.7}_{-1.0}$	1.6 FIXED	9.5/12	–
Q1234+1217	2.51	$4.5^{+9.1}_{-3.1}$	$1.5^{+1.6}_{-0.5}$	3.4/6	
		2.51 FIXED	0.93 ± 0.33	3.8/7	–
MS21340+0018	4.00	$2.7^{+18.3}_{-2.7}$	$0.6^{+1.5}_{-0.3}$	0.71/5	
		4.0 FIXED	0.90 ± 0.45	0.81/6	–
		$6.2^{+6.4}_{-1.7}$	1.6 FIXED	1.62/6	–
SBS0954+495	0.87	$5.2^{+6.8}_{-5.2}$	2.0 ± 2.0	6.5/7	
		0.87 FIXED	0.57 ± 0.30	7.9/8	–
		$4.0^{+1.4}_{-1.0}$	1.6 FIXED	6.6/8	–

Table 6: “Candidate” Cut-off Radio Loud Quasars: Spectral Fits

Quasar	N_{HGal} 10^{20} cm^{-2}	N_H 10^{20} cm^{-2}	α_E	χ^2/dof	prob. ($\Delta\chi^2$)
3C219	1.48	$2.1^{+0.8}_{-1.2}$	0.22 ± 0.40	6.3/22	
		1.48 FIXED	0.05 ± 0.10	6.8/23	–
		$5.7^{+0.7}_{-0.5}$	1.34 FIXED	23.0/23	
PKS1334-127	4.41	$7.1^{+3.0}_{-2.0}$	1.2 ± 0.4	11.0/20	
		4.41 FIXED	0.66 ± 0.13	15.3/21	96.2 %
3C207	4.07	$29^{+30}_{-21.5}$	2.3 ± 1.4	13.6/17	
		4.07 FIXED	0.34 ± 0.16	24.9/18	99.92 %
3C212	3.70	32^{+18}_{-16}	1.9 ± 1.0	14.4/21	
		3.70 FIXED	0.14 ± 0.09	32.0/22	99.997 %
S4 0917+624	3.55	$11.9^{+32}_{-7.9}$	0.46 ± 0.30	5.0/14	
		3.55 FIXED	0.76 ± 0.21	8.25/15	92.6
S4 0917+449	1.51	$2.9^{+1.2}_{-1.0}$	0.79 ± 0.33	17.6/22	
		1.51 FIXED	0.37 ± 0.08	22.1/23	96.6%
4C71.07	2.95	3.3 ± 0.3	0.52 ± 0.09	26.4/29	
		2.95 FIXED	0.43 ± 0.03	28.9/30	–
PKS2351-154	2.39	$5.4^{+3.5}_{-1.2}$	0.87 ± 0.49	12.6/19	
		2.39 FIXED	0.25 ± 0.14	17.3/20	97.0 %
PKS0438-43	1.50	$6.9^{+3.5}_{-1.8}$	$0.70^{+0.27}_{-0.22}$	10.3/22	
		1.5 FIXED	-0.16 ± 0.06	55.4/23	> 99.999
PKS0537-286	2.06	$2.7^{+1.7}_{-1.4}$	0.38 ± 38	16.2/22	
		2.06 FIXED	0.22 ± 0.11	16.8/23	–
		3.8 ± 0.5	0.7 FIXED	17.8/23	–
S40636+680	5.7	5.7 FIXED	-0.1 ± 0.4	10.64/15	
		20^{+10}_{-8}	1.7 FIXED	9.52/15	
PKS2126-158	4.85	$12.9^{+7.2}_{-3.8}$	$0.70^{+0.41}_{-0.29}$	20.6/20	
		4.85 FIXED	-0.03 ± 0.03	49.56/20	> 99.999
PKS1442+101	1.70	$1.9^{+1.2}_{-0.9}$	0.46 ± 0.35	23.2/24	
		1.70 FIXED	0.41 ± 0.10	23.4/23	–
S41745+624	3.31	$6.8^{+0.30}_{-3.0}$	$0.78^{+1.0}_{-0.44}$	14.5/16	
		3.31 FIXED	0.26 ± 0.13	19.1/17	96.8 %

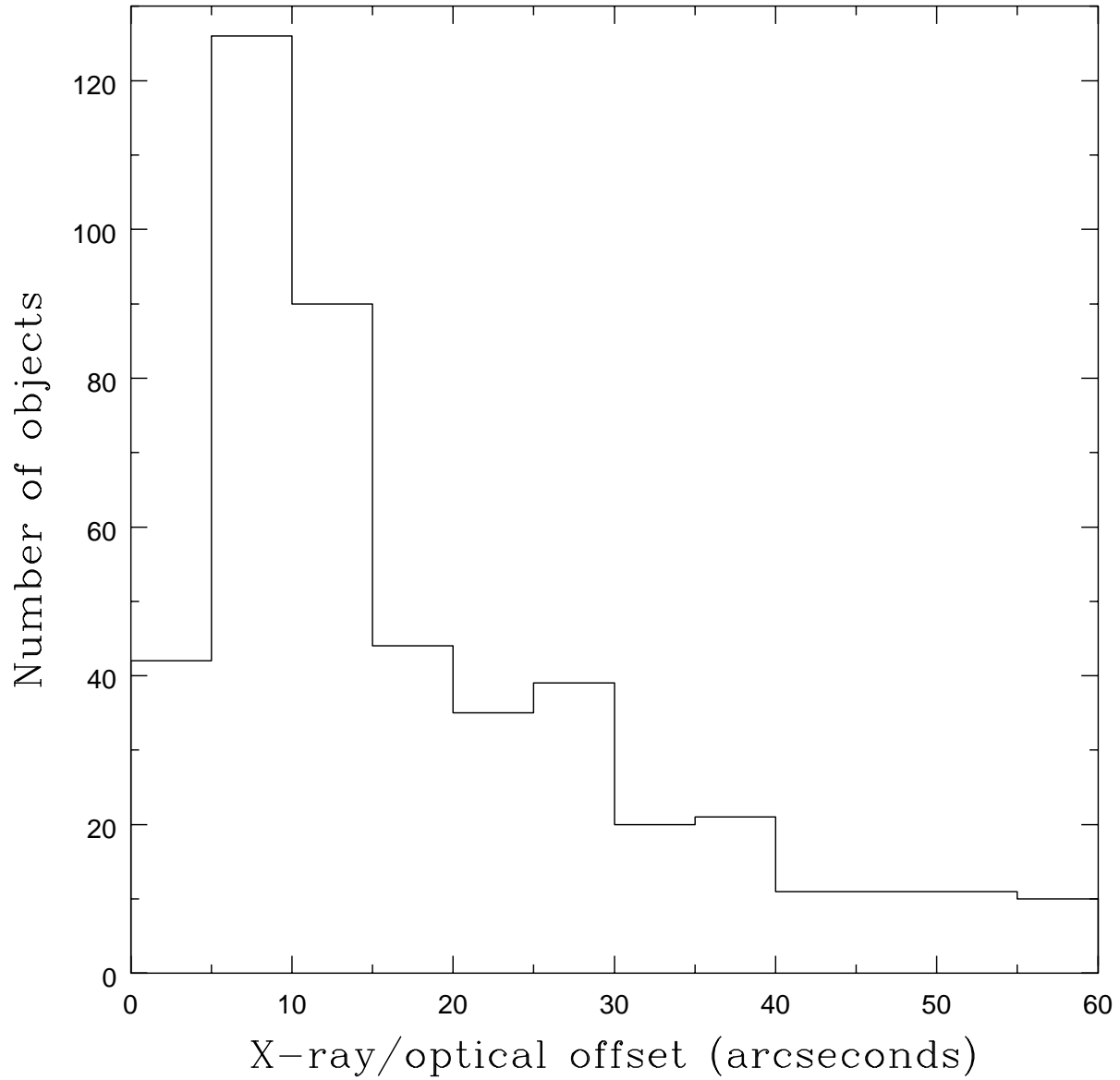


Fig. 1.— The distribution of X-ray/optical offsets for our sources, obtained by cross-correlating the WGA catalog with various optical and radio catalogs with a correlation radius of one arcminute. The mean offset is $\simeq 18$ arcsec. The number of spurious associations is $\lesssim 2$ (see text for details).

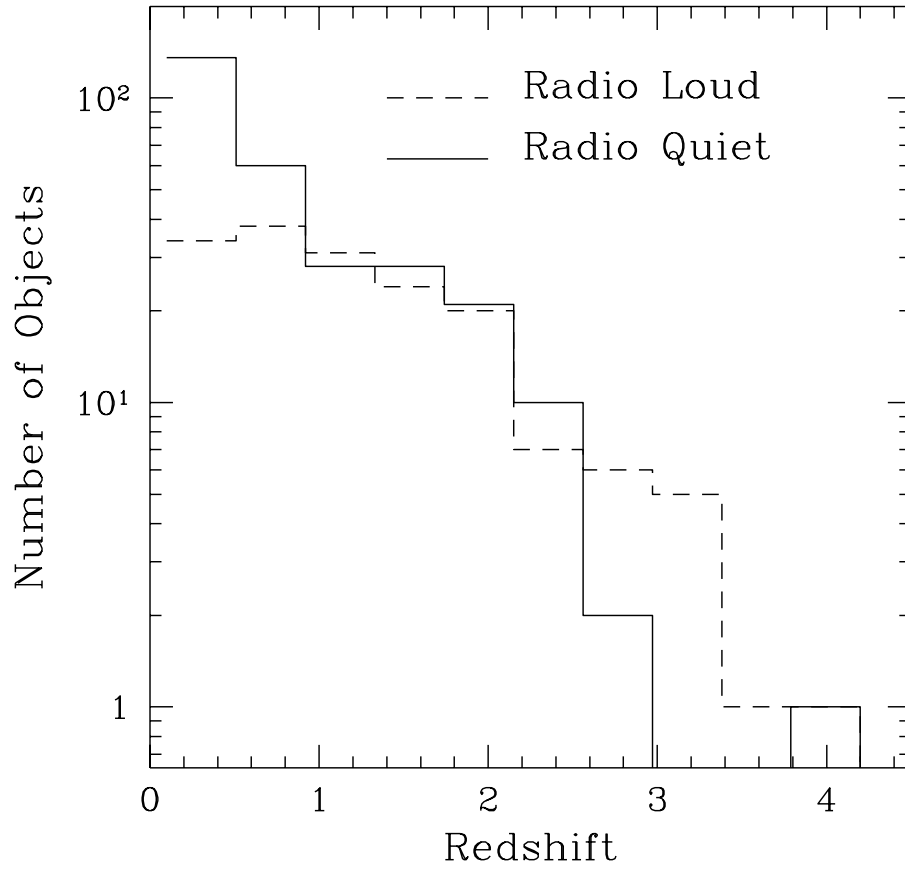


Fig. 2.— The redshift distribution of WGACAT radio-quiet quasars (solid line) and radio-loud quasars (dashed line), used in this paper.

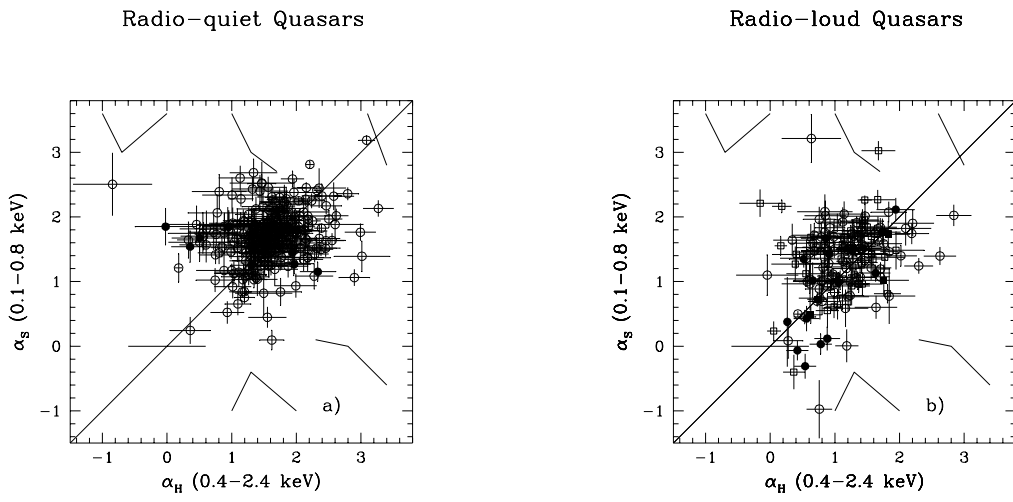


Fig. 3.— The ‘soft’ effective spectral index (α_S) of (a) radio-loud quasars, and (b) radio-quiet quasars plotted against the ‘hard’ effective spectral index (α_H). Radio-loud flat spectrum radio sources are identified by circles, steep radio spectrum sources by squares. High redshift quasars ($z > 2.2$) are shown with filled symbols. Three-point spectra illustrate the radically different spectral shapes in different parts of the diagrams.

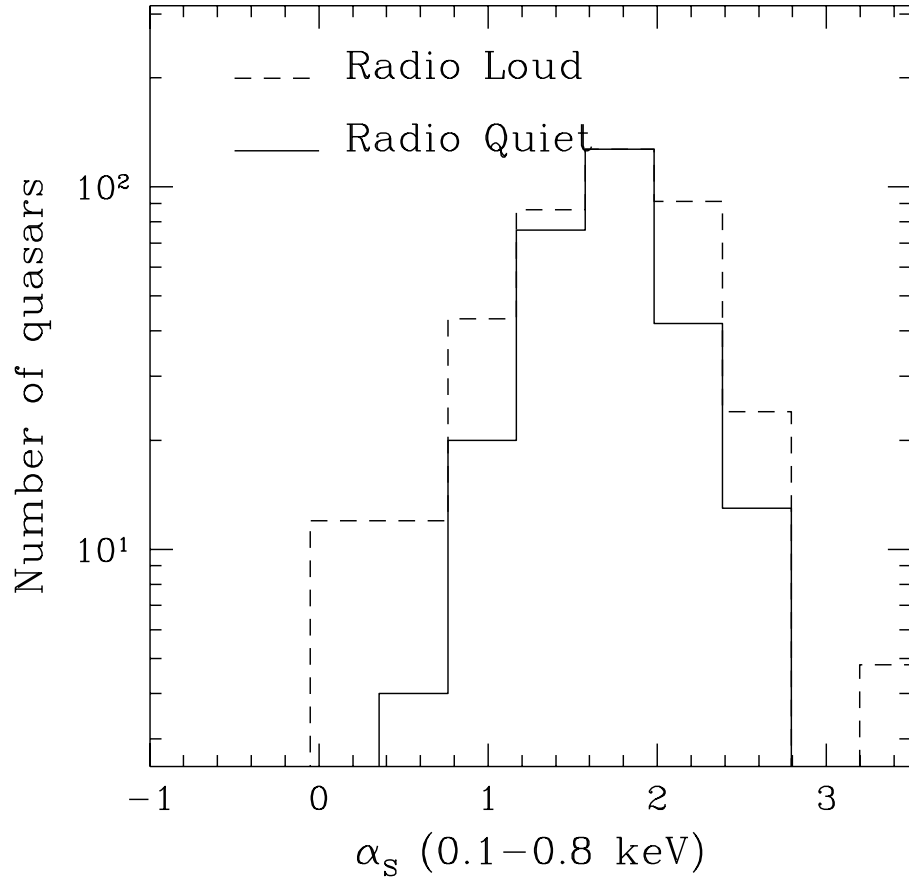


Fig. 4.— The distribution of radio-loud (dashed line) and radio-quiet (solid line) indices about their respective mean α_S . The mean of radio-loud quasars has been offset to coincide at $\alpha_S = 1.7$ with that of radio-quiet quasars. The radio-loud distribution has been normalized to the maximum of the radio-quiet distribution.

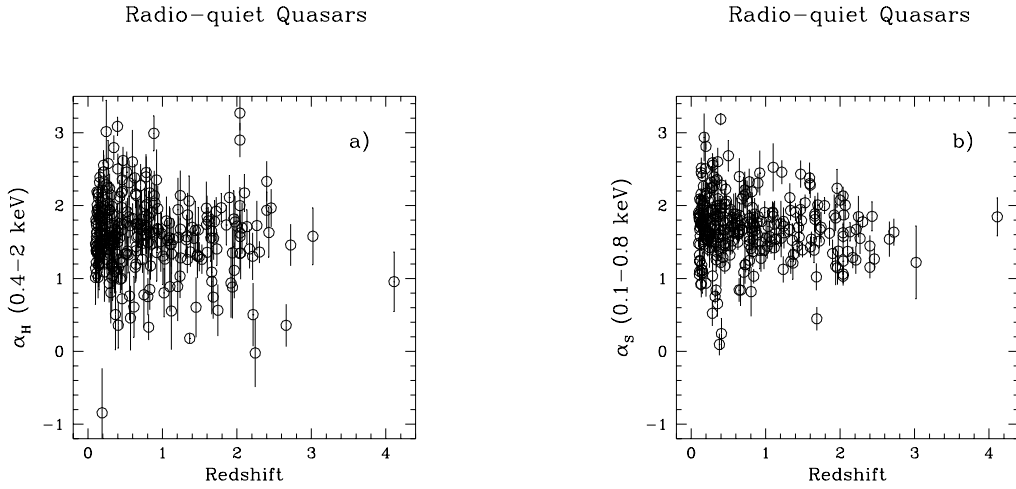


Fig. 5.— α_H (a) and α_S (b) plotted against the redshift for radio-quiet quasars.

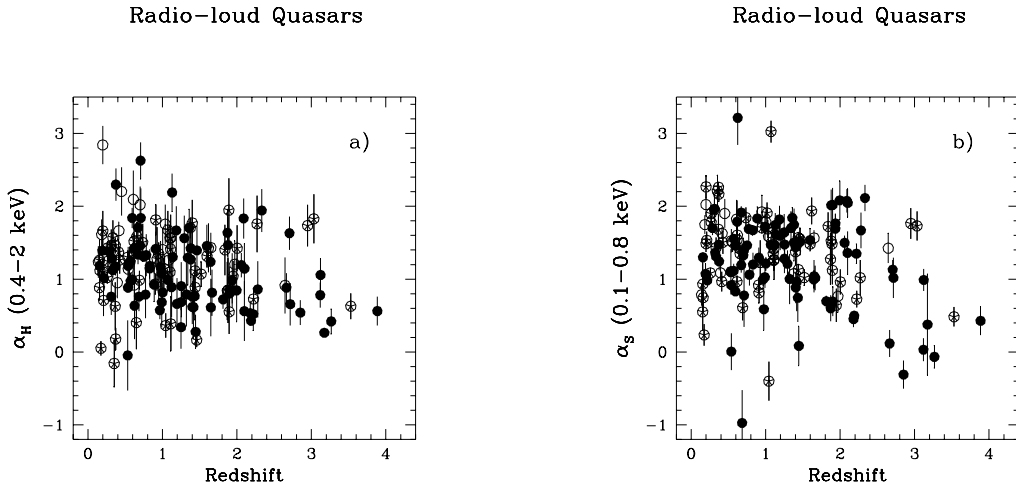


Fig. 6.— α_H (a) and α_S (b) plotted against the redshift for radio-loud quasars. Filled circles identify flat radio spectrum quasars. Starred circles identify steep radio spectrum quasars.

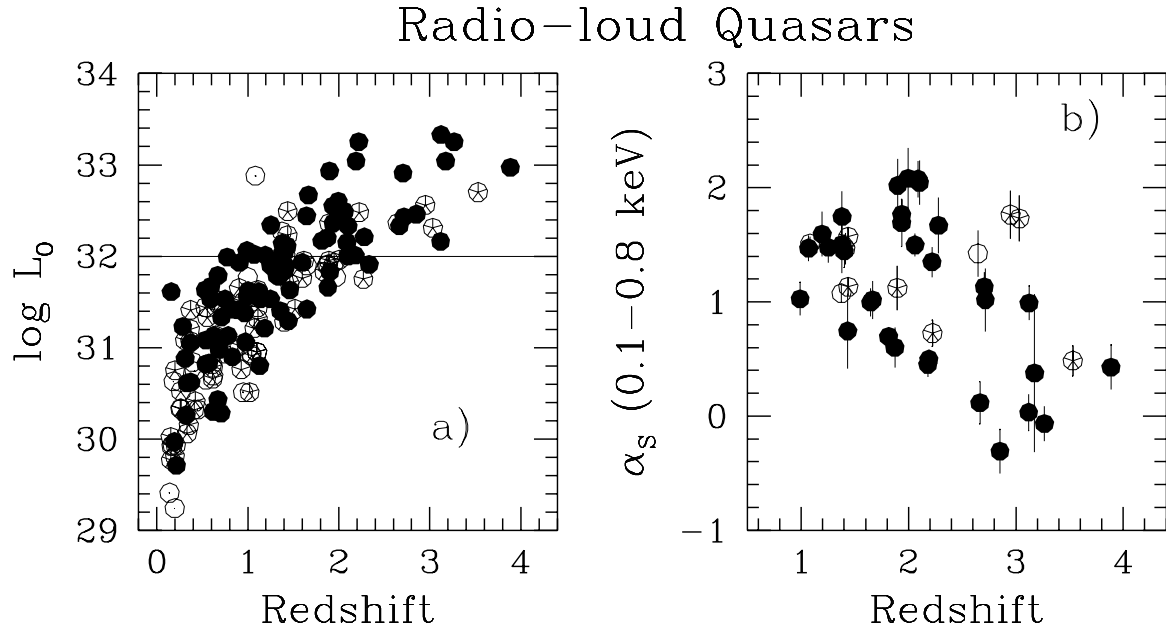


Fig. 7.— (a) The redshift–optical luminosity correlation for radio loud quasars. (b) The soft spectral index α_S –redshift correlation for radio-loud quasars with high optical luminosity ($> 10^{32} \text{ erg s}^{-1}$).

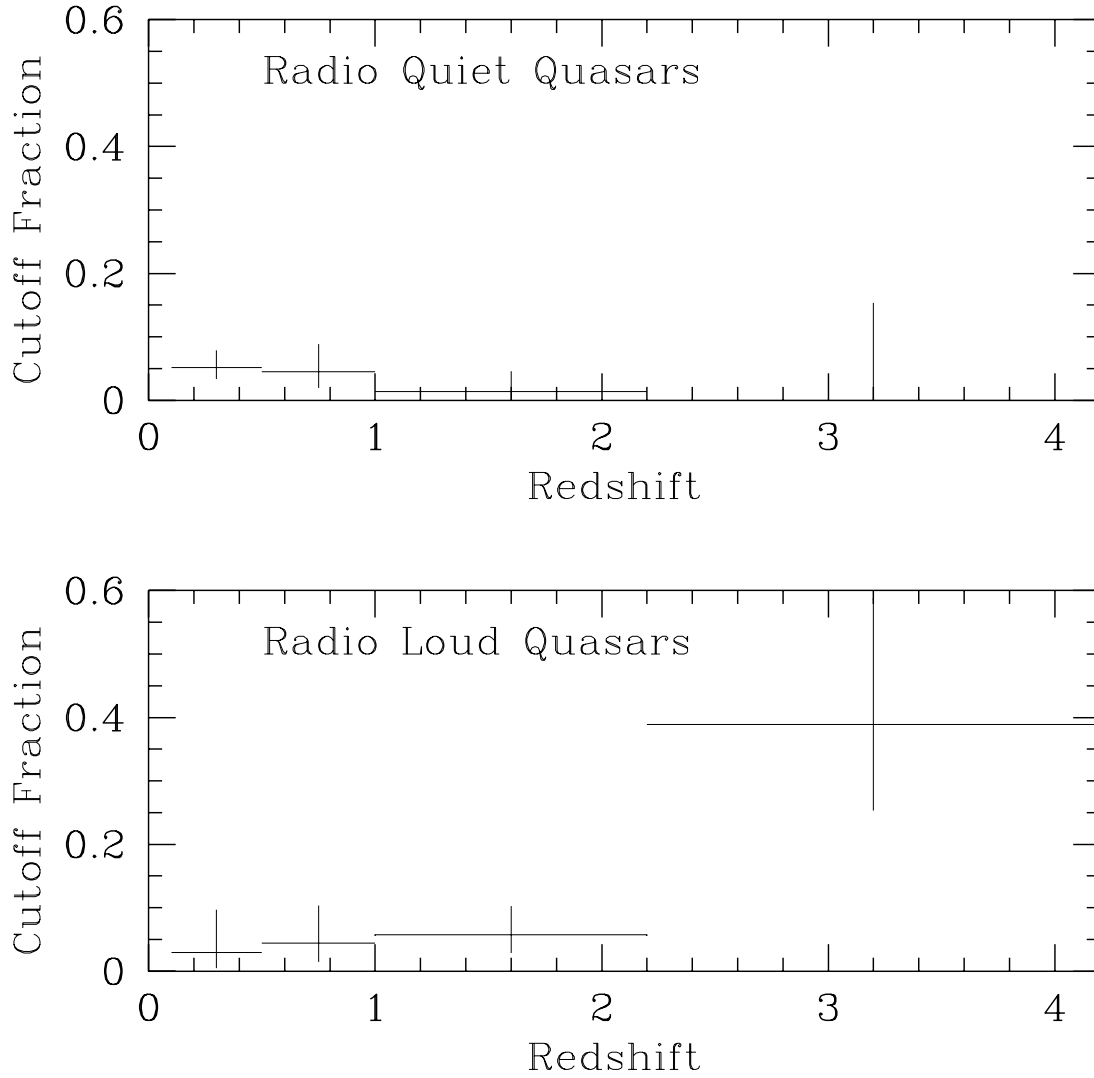


Fig. 8.— The fraction of “candidate” cut-off quasars as a function of the redshift for radio quiet quasars (upper panel) and radio-loud quasar (bottom panel).